(1) For the same fire insulation thickness, Point A5 experiences higher temperatures than Point A6 at Section A for the strengthened beams during fire, since Point A5 is located next to the corner of the beams, where the fire exposure is two-sided. Experimental results in literature [12] have shown that the shear strength of adhesive between the concrete and the CFS almost lost completely at about 150 ℃ [302 ℉]. According to the results shown in Table 2, it can be concluded that the complete loss of interaction between the CFS and the concrete occurred at about 25 min and 37 min of the fire exposure for the fire insulation thickness of 10 mm [0.394 in] (Beams L1 and L4) and 20 mm [0.788 in] (Beams L2, L3, L5, L7, L8), respectively.

(2) For the strengthened beam L1 and the unstrengthened beam L6, the temperature-time curves of Points B7 and B8 at Section B are close to that recorded at Point A2 at Section A, indicating that the temperature distributions related to different cross sections along beam span are consistent on the whole. However, this trend may be changed due to concrete spalling occurs randomly. For instance, the temperature-time curves of Points B7 and A2 at different sections for the strengthened beam L8 are close to each other, but the temperature at Point B8 begins to increase gradually after 20 min of the fire exposure, due to local concrete spalling.

(3) For the strengthened beams L1~L5, L7 and L8, the recorded temperature at Point A1 related to the main reinforcement is less than that at Point A2 related to the steel stirrup firstly, due to the protection provided by the fire insulation at beam soffit, but the former is gradually close to and even larger than the latter with increasing of the heating time, attributing to the destroy and falling off of the insulation during the fire exposure.

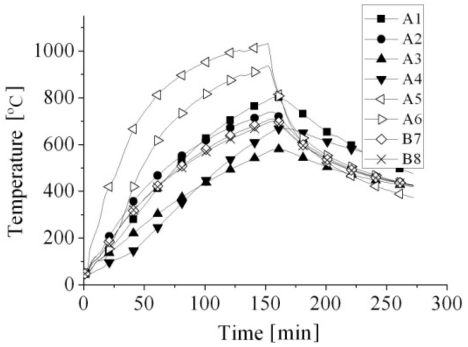

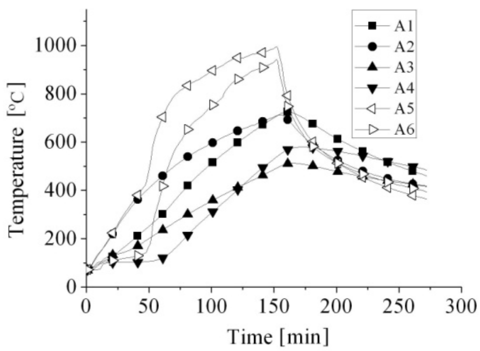

(a) L1

(b) L2

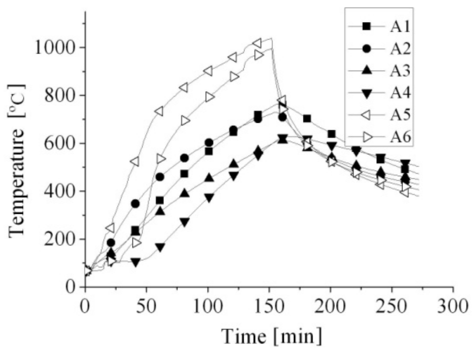

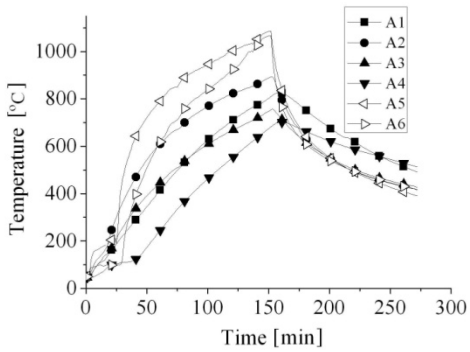

(c) L3

(d) L4

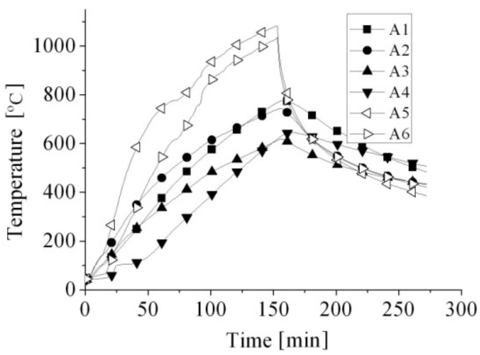

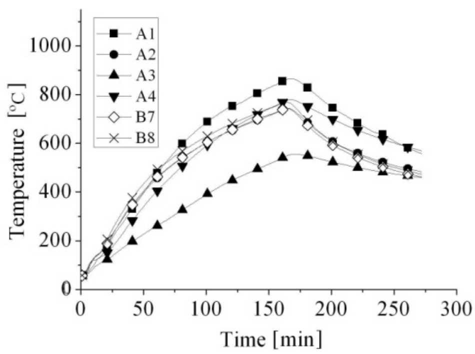

(e) L3

(f) L4

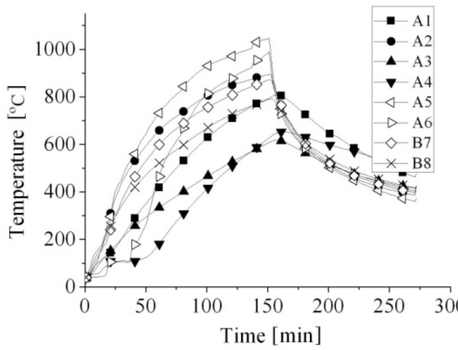

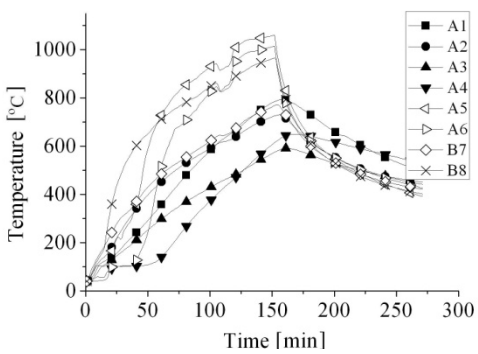

(g) L7

(h) L8

Fig.7 Measured temperatures as a function of the fire duration (1 ℃=(1 ℉-32)/1.8)

Table 3 Heating times related to 150 ℃ [302 ℉] for Points A5 and A6

Specimen No.	Insulation thickness / mm	Point A5		Point A6		Mean time related to 150 ℃ for Point A6 / min
		Time / min	Temperature /℃	Time / min	Temperature /℃	
L1	10	5	148.60	21	154.09	25
L4	10	6	154.09	30	147.40	
L2	20	12	151.69	48	144.09	37
L3	20	13	148.89	33	149.59	
L5	20	15	156.70	23	152.19	
L7	20	13	151.00	38	147.89	
L8	20	20	151.18	43	151.18	

1 mm=0.0394 in; 1 ℃=(1 ℉-32)/1.8

3.3 Structural behavior

Deflection

Fig.8 shows the measured deflections as a function of the fire duration at Locations ①, ② and ③ (see Fig.4) for the specimens, and Fig.9 shows a comparison of the measured deflections at mid-span as a function of the fire duration for the specimens. It can be seen from these figures that:

(1) The recorded deflection at Location ② (i.e., mid-span) increases more quickly than that at Locations ① and ③, especially in the late stage of the heating phase. As expected, the deflections at the symmetrical Locations ① and ③ are close to each other on the whole.

(2) The deflections of the strengthened beams show a slight decreasing at about 50 min in the cooling phase, indicating a slight recovery of the beams' stiffness after 50 min of cooling.

(3) In the heating phase of 150 min, the mid-span deflections of the strengthened and insulated beams L3, L7 and L8 are very similar to each other and larger than that of the unstrengthened beam L6. This is attributed to the fact that for the same load ratio of 0.3, the strengthened beams with larger ultimate capacity carried larger applied load than the unstrengthened beam, while the difference between the stiffness of the strengthened beams and that of the unstrengthened beam was limited.

(4) In the heating and cooling phases, for the strengthened beams L4 and L1 with the same load ratio and fire insulation thickness (10 mm [0.394 in]) and with different beam end restraints, the mid-span deflection of the former is always larger than that of the latter after a heating of 10 min, indicating that the restraints at beam ends have some influence on the deformation of the strengthened beams with thinner fire insulation at high temperature. However, for the strengthened beams L5 and L2 with the same load ratio and fire insulation thickness (20 mm [0.787 in]) and with different beam end restraints, their mid-span deflections are close to each other, implying that the influence mentioned above decreases with the increasing of the fire insulation thickness.

(5) In the heating and cooling phases, the maximum mid-span deflections of all the specimens ranging from 12 mm [0.472 in] to 16 mm [0.630 in] are much smaller than the value of *L*/20 (*L* is the beam span) which is specified in the testing guideline for simply supported beams [13], indicating that the loss of interaction between the CFS and the concrete occurred early in the fire exposure, but the restrained beams could still maintain satisfactory fire behavior in both the heating phase of 150 min and the cooling phase of 120 min. Considering the fact that there is no general agreement on the most suited failure criterion for restrained beams at high temperature, the failure criterion related to the simply supported beams is adopted here to give a preliminary judgement.

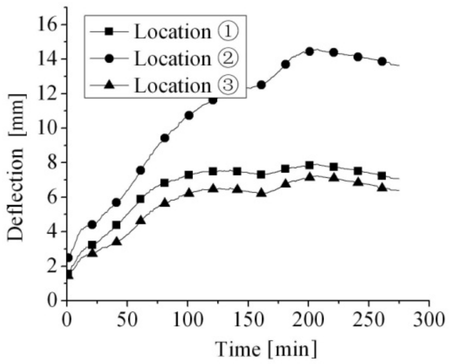

(a) L1

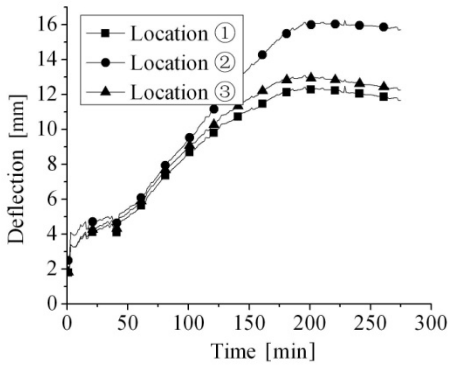

(b) L2

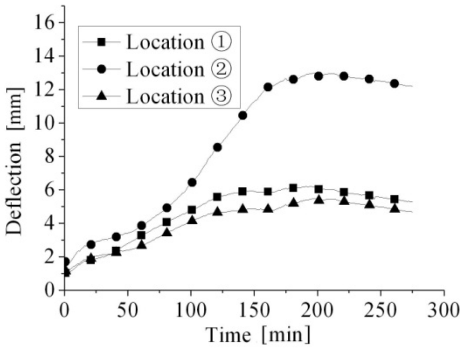

(c) L3

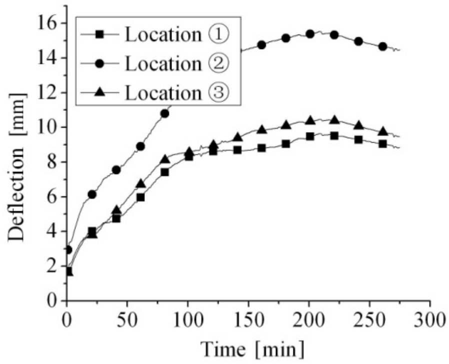

(d) L4

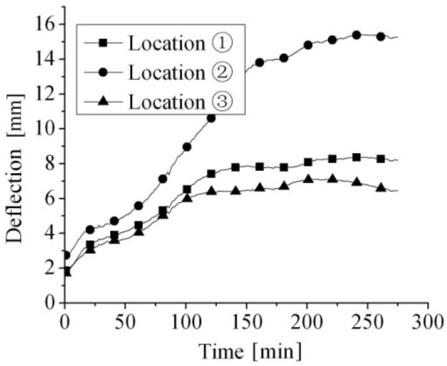

(e) L5

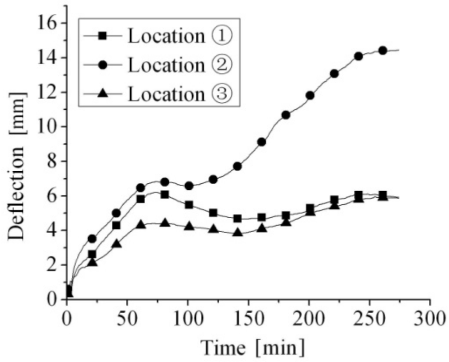

(f) L6

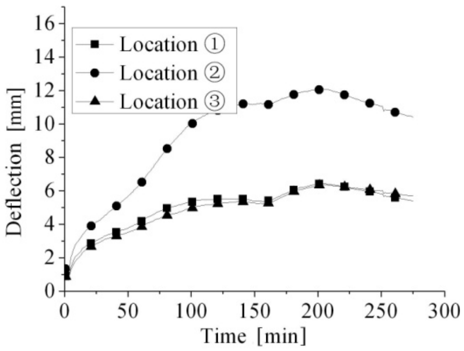

(g) L7

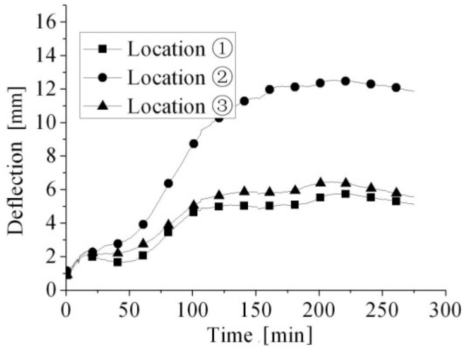

(h) L8

Fig.8 Measured deflections as a function of the fire duration (1 mm=0.0394 in)

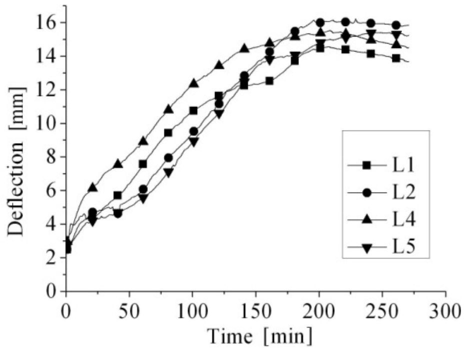

(a) L1, L2, L4, L5

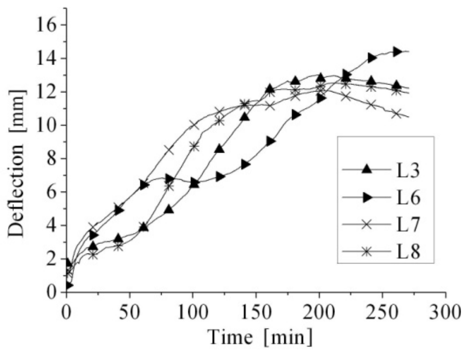

(b) L3, L6, L7, L8

Fig.9 Measured deflections at mid-span as a function of the fire duration (1 mm=0.0394 in)

Axial elongations

Fig.10 shows a comparison of the measured axial elongations as a function of the fire duration for all the specimens in fire with cooling phase, which measured by the LVDTs at Locations 1 and 2 as shown in Fig.3(a). Table 3 gives a summary of the test results of the specimens. From Fig.10 and Table 3 it can be seen that:

(1) The axial elongations of the specimens increase gradually with the increasing of heating time, then recover to a certain degree during the cooling process, and the maximum axial elongations occurred at about 10 min of the cooling phase.

(2) For the specimens L3, L6, L7 and L8 with a load ratio of 0.3, the maximum axial elongations of the former three ones are larger than that of the latter, due to the axial restraint stiffness ratio of Beam L8 larger than that of Beams L3, L6 and L7. Similarly, for the specimens L1, L2, L4 and L5 with a load ratio of 0.5, the maximum axial elongations of the former two ones are larger than those of the latter two ones.

(3) Although the load ratio and the axial restraint stiffness ratio of Beam L1 are, respectively, the same as those of Beam L2, the maximum axial elongation of the former is slightly larger than that of the latter, due to a thinner fire insulation of Beam L1 which resulting in higher temperatures in this beam. Similarly, the maximum axial elongation of Beam L4 is slightly larger than that of Beam L5 too.

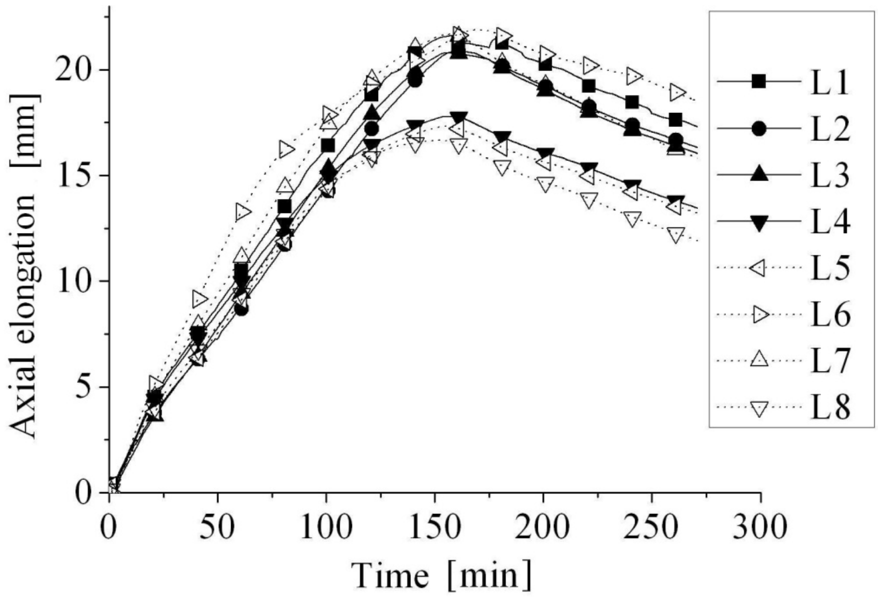

Fig.10 Measured axial elongations as a function of the fire duration (1 mm=0.0394 in)

Table 4 Summary of test results

Specimen No.	Max. axial elongation /mm	Axial forces			Bending moments at beam ends		
		Mean value of max. axial forces obtained at left and right beam ends /kN	Mean value of max. additional axial forces obtained at left and right beam ends [a] /kN	Max. axial force ratio [b]	Mean value of max. bending moments obtained at left and right beam ends /kN.m	Mean value of max. additional bending moments obtained at left and right beam ends [c] /kN.m	Max. bending moment ratio [d]
L1	21.65	205.6	239.2	0.054	83.07	55.79	0.96
L2	20.86	171.6	209.1	0.045	86.01	53.20	1.00
L3	20.78	200.7	225.3	0.053	66.49	43.95	0.77
L4	17.78	341.6	389.3	0.090	93.96	55.94	1.09
L5	17.32	333.9	378.8	0.088	89.92	53.71	1.04
L6	21.89	235.4	250.8	0.062	79.48	70.29	0.92
L7	21.67	210.9	230.5	0.056	72.41	57.52	0.84
L8	16.67	344.9	370.2	0.091	69.07	47.02	0.80

1 mm=0.0394 in; 1 kN = 0.225 lbf

Notes: [a] additional axial force is defined as the difference between the axial force at high temperature and that at room temperature.

[b] maximum axial force ratio is defined as the ratio of the mean value of maximum axial forces to $f_c A$, where A is the beam sectional area, and f_c is the compressive strength of concrete at room temperature.

[c] additional bending moment is defined as the difference between the bending moment at high temperature and that at room temperature.

[d] maximum bending moment ratio is defined as the ratio of the mean value of maximum bending moments to the flexural capacity of the unstrengthened beam at ambient temperature.

Axial forces in beams

Fig.11 shows the measured axial forces as a function of the fire duration at beam ends for all the specimens. It can be seen from Fig.11 and Table 3 that:

(1) The axial force obtained at the left beam end is consistent with that at the right beam end on the whole; the axial forces increase gradually with an increasing of the heating time, then recover slightly during the cooling process, and the maximum axial forces occurred at about 10 min of the cooling phase. It should be noted that the monotonic increasing of the axial forces during the heating phase occurs only for the heating time of 150 min, in this case the beam's thermal elongation is significant and the reduction of the beam's axial stiffness is limited. But in the case that the heating time is much larger (e.g., monotonic heating), the axial forces maybe decrease in the heating phase, due to the great reduction of the beam's axial stiffness ensuing from the seriously thermal damage.

(2) For the specimens L3, L6, L7 and L8 with a load ratio of 0.3, the maximum additional axial forces of the former three ones are significantly less than that of the latter, due to the axial restraint stiffness ratio of Beam L8 larger than that of Beams L3, L6 and L7. Similarly, for the specimens L1, L2, L4 and L5 with a load ratio of 0.5, the maximum additional axial forces of the former two ones are significantly less than those of the latter two ones.

(3) Although the load ratio and the axial restraint stiffness ratio of Beam L1 are, respectively, the same as those of Beam L2, the mean value of the maximum additional axial forces obtained at the left and right beam ends of L1 is larger than that of L2, due to a thinner fire insulation of Beam L1 which results in higher temperatures in this beam and larger axial thermal elongation. Similarly, the mean

value of the maximum additional axial forces obtained at the left and right beam ends of Beam L4 is larger than that of Beam L5, and the mean value of the maximum additional axial forces obtained at the left and right beam ends of the uninsulated Beam L6 is larger than that of the insulated Beams L3 and L7.

(4) The largest value of the maximum axial force ratios in Table 3 is 0.091. It should be pointed out that the maximum axial force ratio in this Table is defined as the ratio of the mean value of maximum axial forces obtained at left and right beam ends to the beam's axial bearing capacity at room temperature, it is no doubt that the maximum axial force ratio will significantly increase in the case that the beam's axial bearing capacity at elevated temperature is adopted as the denominator. After the heating phase of 150 min and the cooling phase of 120 min, residual axial compressive forces still exist in all the specimens.

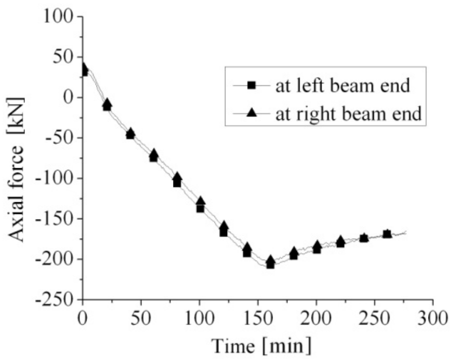

(a) L1

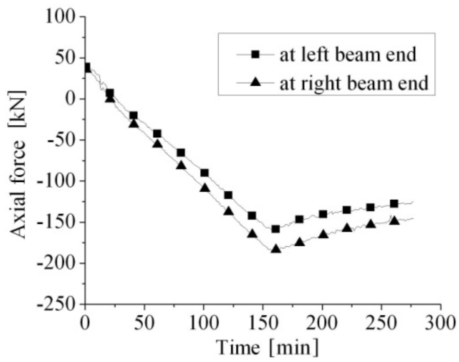

(b) L2

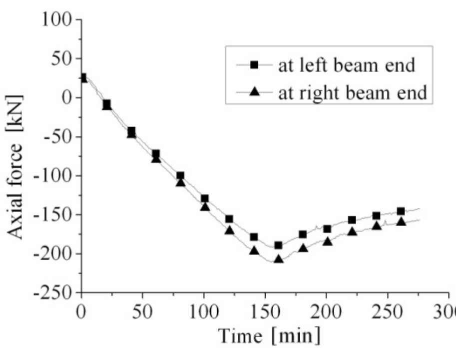

(c) L4

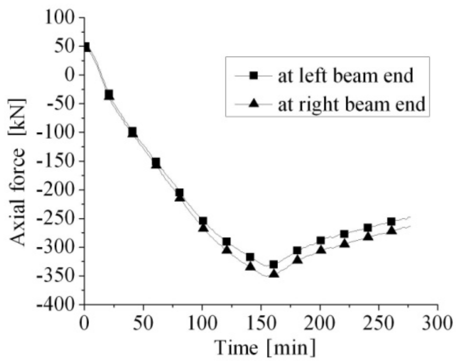

(d) L5

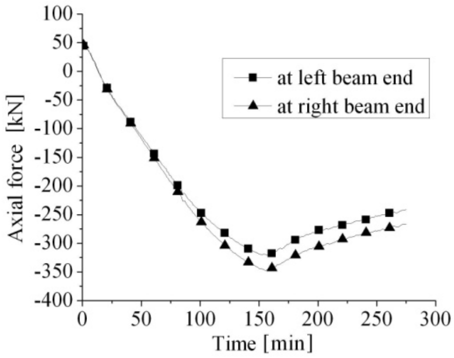

(e) L4

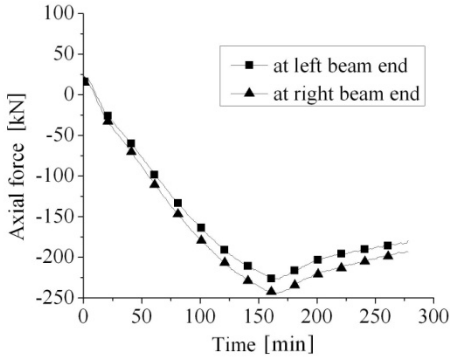

(f) L5

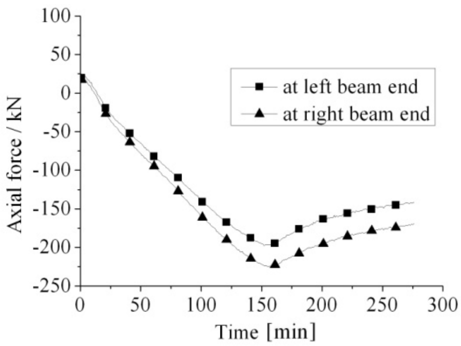

(g) L7

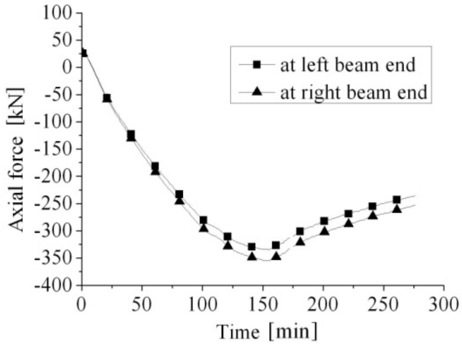

(h) L8

Fig.11 Measured axial forces as a function of the fire duration (1 kN=0.225 lbf)

Bending moments at beam ends

Fig.12 shows the measured bending moments at beam ends as a function of the fire duration for all the restrained specimens. It can be seen from Fig.12 and Table 3 that:

(1) The bending moments at the left and right beam ends during a fire with cooling phase increase gradually first and then recover significantly. This is due to that: (a) At the early stage of the heating phase, the thermal expansion of the concrete close to the heated beam soffit is larger than that close to the unheated surface of the beam (i.e., top surface of the beam), resulting in the additional compressive stresses in the concrete close to the beam soffit larger than those close to the unheated surface of the beam. The nonuniform distribution of these additional compressive stresses induces additional hogging moments at beam ends, resulting in an increasing of the bending moments at the left and right beam ends. (b) At the late stage of the heating phase, the additional compressive stresses in the concrete close